Liquefaction of Saturated Sand Deposits Under Nonuniform Vertical Stresses

Tetsuro YAMAMOTO*, Sukeo ŌHARA** and Mitsuo ISHIKAWA***

(Received July 5, 1993)

Abstract

In order to clarify the characteristics of liquefaction and liquefaction-induced settlement of saturated sand deposits of which the vertical stresses are different partially such as those below and near overburden structures, a series of shaking table tests are performed on the model sand layer prepared in three Kjellman's type simple shear boxes. The model sand layer consists of three saturated sand layers of which the effective vertical stresses σ'_{vo} are 10.4kPa, 30.0kPa and 49.6kPa respectively, and is called model (1) hereafter. Also, the same tests are carried out on four models (2) to (5) consisting of two sand layers having different RVS-values. Here RVS$=(\sigma'_{vo})_s / (\sigma'_{vo})_l$, in which $(\sigma'_{vo})_s$ and $(\sigma'_{vo})_l$ represent lower and higher vertical stresses of two respective sand layers.

It is found from the tests that in the case of seismic coefficient $k_h \geqq 0.15$, irrespective of the RVS-values and in the case of $k_h < 0.15$ and RVS$\geqq 0.5$, all sand layers of the models liquefied almost simultaneously. On the contrary, in the case of $k_h < 0.15$ and RVS< 0.5, the sand layer of $(\sigma'_{vo})_s$ liquefied easily due to the effect of pore water pressure induced in the sand layer of $(\sigma'_{vo})_l$, though the sand layer of $(\sigma'_{vo})_l$ didn't occur to liquefy. Namely, it was concluded that the liquefaction characteristics of such model sand layers were affected by the RVS-value and the acceleration level of vibration.

Furthermore, it is shown that the amount of the liquefaction-induced settlement of the model sand layer increases remarkably in the range of lower vertical stresses and takes almost a constant value as the vertical stresses increase.

Introduction

It has been reported that overburden structures such as embankments, earth dams and civil engineering structures have been damaged by liquefactions of saturated sandy deposits below those structures during earthquakes (Fact-finding committee on the Niigata earthquake damage of JSCE[1], Seed et al.[2], Sasaki et al.[3]).

However, up to now, as will be mentioned below only a few experimental studies have been made on the liquefaction characteristics of saturated sand deposits of which the vertical stresses differ partially such as those below and near the overburden structures or the civil engineering structures. All of the tests are carried out using the

*Department of Civil Engineering
**Ube Technical College
***Graduate student, Department of Civil Engineering
©1993 The Faculty of Engineering, Yamaguchi University

sand boxes fixed on the shaking tables and the model structures are classified into two types. One is of the rigid model structure resting on relatively loose saturated sand layer (Yoshimi and Tokimatsu[4)~6)], Ishihara and Matsumoto[7)]). The other is of the model sand embankment founded on relatively loose saturated sand layer (Koga and Matsuo[8)], Abe and Kusano[9)]). We will outline their test methods and results below.

Yoshimi and Tokimatsu[4)~6)] measured the amount of settlement of the rigid model structure placed on the sand layer of relative density Dr=60% and the pore water pressures u induced in the sand layer during the vibration. A size of the sand layer prepared in the sand box is 130cm in length, 30cm in depth and 19.75cm in width. Two kinds of model structures of the load intensity q =2.0 and 6.0kPa with 20cm in length and 19.7cm in width were used. Free vibration with a maximum acceleration amplitude 100gal was applied to the sand layer.

Fig. 1 shows an example of the distribution of the maximum pore water pressure ratio $(u/\sigma'_{vo})_{max}$ induced in the sand layer during the vibration[4)~6)]. It is noticed in Fig. 1 that $(u/\sigma'_{vo})_{max}$ at Points P2, P3, P5 and P6 in the sand layer near the structure are about 1.0, that is, those points liquefied. On the contrary, $(u/\sigma'_{vo})_{max}$ at Points P1 and P4 in the sand layer below the structure are about 0.4, that is, those points didn't liquefy. The authors mentioned that the reason for this result is that since larger effective vertical stress induced in the sand layer below the structure due to its own weight as compared with that induced in the sand layer near the structure, the sand layer below the structure hardly occurs to liquefy.

Ishihara and Matsumoto[7)] studied the dynamic bearing capacity of the saturated sand layer of Dr=25% on which the model foundation was placed. In the tests, the pore water pressures at five points shown in Fig. 2 (a) were measured. The sand layer was prepared in the sand box with 4.0m in length, 1.0m in height and 1.0m in width. The four model foundations of q=7.1, 8.7, 10.5 and 12.9kPa with 0.5m long and 0.5 m wide were used. The acceleration of vibration was increased gradually. The authors obtained the relation between the pore water pressure u induced in the sand layer and the value of q, at the time when the acceleration of vibration became large

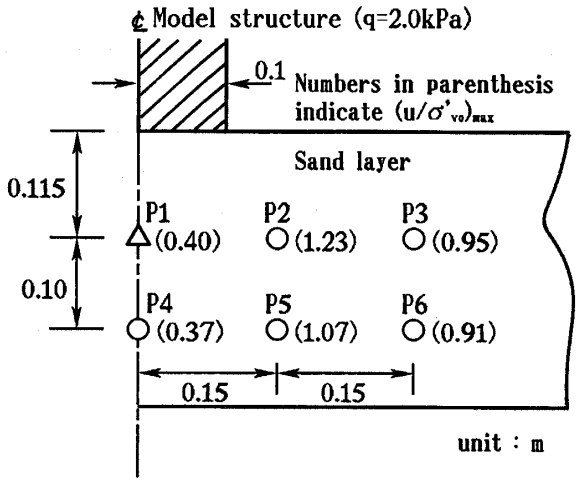

Fig. 1 Maximum pore water pressure ratio $(u/\sigma'_{vo})_{max}$ induced in the sand layer below and near the model structure with q=2.0kPa during vibration (After Yoshimi and Tokimatsu (1975))

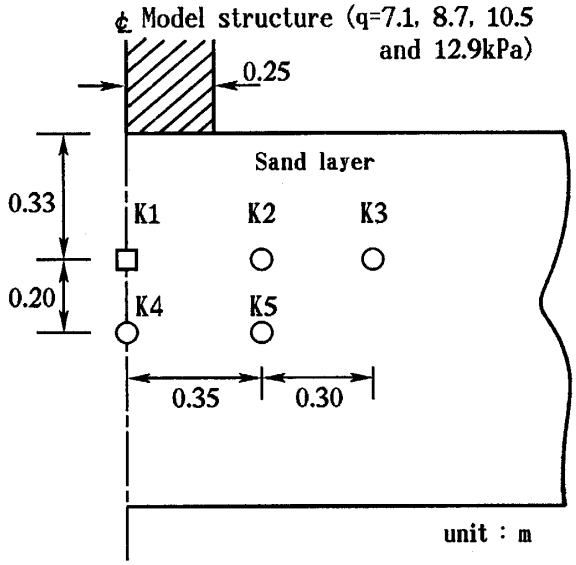

Fig. 2 (a) Measuring points of pore water pressures induced in the sand layer during vibration (After Ishihara and Matsumoto (1975))

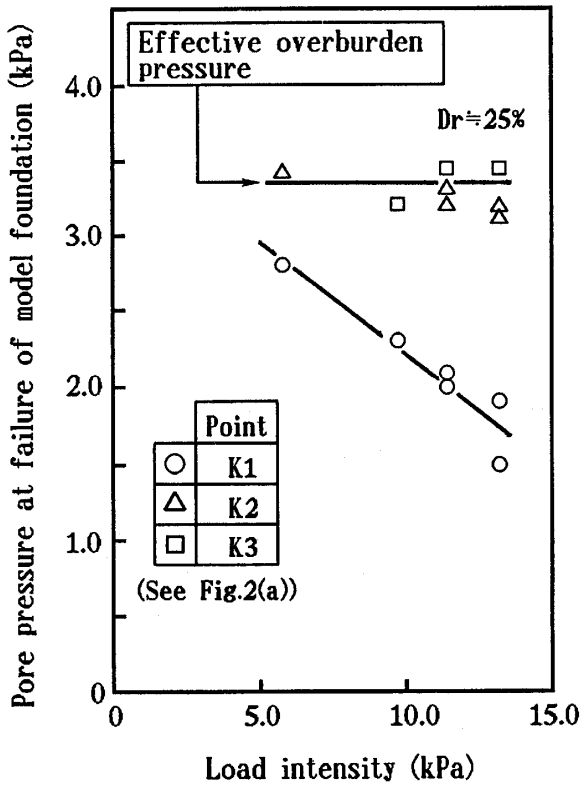

Fig. 2 (b) Pore pressure induced in each model foundation at the time settlement begins (After Ishihara and Matsumoto (1975))

enough to cause the settlement of the model foundation as shown in Fig. 2 (b). The acceleration amplitude in this case is about 40gal. It is seen from this figure that this test result is similar to Yoshimi and Tokimatsu's test result. Namely, Point K1 in the sand layer below the structure doesn't liquefy, though Points K2 and K3 in the sand layer near the structure liquefy. Also, it is noticed that the value of u/σ'_{vo} of the sand layer below the structure decreases as the value of q increases. Their explanation for this test result is the same as Yoshimi and Tokimatsu's one.

On the other hand, it has been emphasized that the liquefaction resistance of saturated sand decreases slightly with increasing a confining pressure[10),11)]. These results were obtained from the liquefaction tests using cyclic triaxial test apparatus. As shown in Fig. 8 , the same result as that of them was obtained in our experiments.

Therefore, it seems to be difficult to accept their conclusions that the sand layer below the structure does not liquefy due to the increase of effective vertical stress induced in the sand layer by the own weight of the structure.

Koga and Matsuo[8)] carried out the vibration tests on six model embankments founded on the sand layer with depth of 0.4m. The model embankments are height 0.2m, a crest width of 0.2m and side slopes of 1 : 2. Fig. 3 shows the contour of u/σ'_{vo} in the sand layer just after the vibration obtained from Test 1. Sinusoidal acceleration with $k_h=0.22$ and period $T=0.4$sec was used in this test. From this

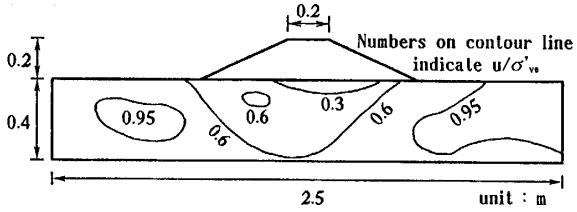

Fig. 3 Contour of pore water pressure ratio u/σ'_{vo} just after the shaking (Test 1 at 220gal shaking; t=9sec) (After Koga and Matsuo (1990))

figure the authors concluded that the sand layer below the embankment doesn't liquefy, while the sand layer with free surface near it liquefies. They mentioned that this is due to the difference between the vertical and horizontal stresses in the sand layers below the embankment and with free surface.

The test result similar to those is obtained by Abe and Kusano[9] who performed the vibration tests of the model embankment founded on the saturated sand layer. The model sand embankment is thickness of 0.4m, a crest width of 0.2m and slopes of 1 : 2.

In this paper, in order to clarify the liquefaction characteristics of the saturated sand deposit below and near a structure, as shown in Fig. 4, the shaking table tests were performed on the model (1). This model consists of three individual soil elements of which the vertical stresses are 10.4kPa, 30.0kPa and 49.6kPa, and the neighbor elements are connected by the hard pipes in order to flow pore water freely. That is, the sand layers of $\sigma'_{vo}=10.4$kPa and 30.0kPa correspond to the soil elements near the structure, and the sand layer of $\sigma'_{vo}=49.6$ kPa corresponds to the soil element below the structure. Although a small initial shear stress may be induced on the sand layer of $\sigma'_{vo}=30.0$kPa, we will neglect its effect on the liquefaction characteristic of the sand layer. The amount of liquefaction-induced settlement of this model was also investigated.

In order to clarify the reason why the sand layer near the structure easily liquefies and the sand layer below the structure doesn't liquefy, the same tests were performed on the models (2)~(5) consisting of two sand layers having the different vertical stress ratios RVSs, which is defined by Eq. (1).

$$RVS=(\sigma'_{vo})_s/(\sigma'_{vo})_1 \qquad (1)$$

in which $(\sigma'_{vo})_s$ and $(\sigma'_{vo})_1$ represent lower and higher vertical stresses, respectively. The values of σ'_{vo} and RVS of these model sand layers are summarized in Table 1.

On the basis of these test results we will discuss the difference of the increase of pore water pressures induced in the model saturated sand layers during the vibration in conjunction with the RVS-values and the magnitude of k_h.

Test Apparatus

In this study, three Kjellman's type simple shear boxes shown in Fig. 5 was used.

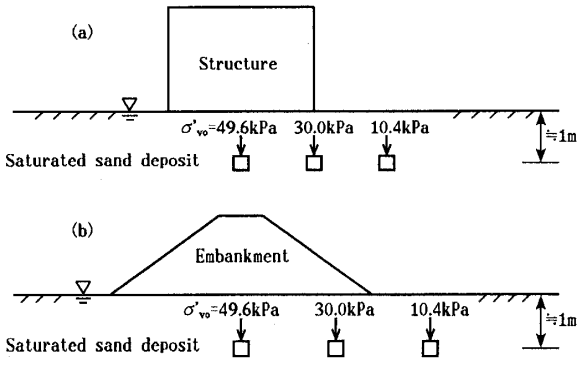

Fig. 4 Model (1) consisting of three sand layer elements below and near a structure or an embankment

Table 1 Kind of model sand layers

Model	σ'_{vo}(kPa)				RVS
	10.4	20.0	30.0	49.6	
1	○	—	○	○	0.35
2	○	○	—	—	0.52
3	○	—	○	—	0.35
4	○	—	—	○	0.21
5	—	—	○	○	0.60

As shown in this figure, by connecting the neighboring two sand layers by the hard pipes ⑩ with innner diameter of 8mm which was filled with the pore water, the model (1) consisting of three sand layers of which the vertical stresses σ'_{vo} are 10.4kPa, 30.0kPa and 49.6kPa respectively, was prepared.

Because the details of the shear box were described in our previous studies[12)~14)], we shall describe them only briefly below. To prevent the lateral expansion of the sand layer and to induce the simple shear deformation, six polyvinyl chloride rings ③ are stacked around the sand layer, which was covered with the rubber membrane ⑤ of 1.0 mm in thickness. A size of each ring is 1cm in thickness, and inner and outer diameters are 30.2cm and 35.0cm, respectively.

Preparation of Model Sand Layer

Three saturated Toyoura sand layers were prepared by carefully pouring wet sand into a water-filled rubber membrane firstly. Then the sand layers were lightly compacted by a tamper to obtain the sand layers with Dr=55%. The sand layer size is 30cm in diameter and about 6cm in height.

The physical properties of Toyoura sand are as follows. $G_s=2.646$, $D_{max}=0.85$mm, $D_{50}=0.16$mm, $U_c=1.4$, $e_{max}=0.944$, $e_{min}=0.610$.

Thereafter, the required set of steel plate weight and lead ring weight were placed

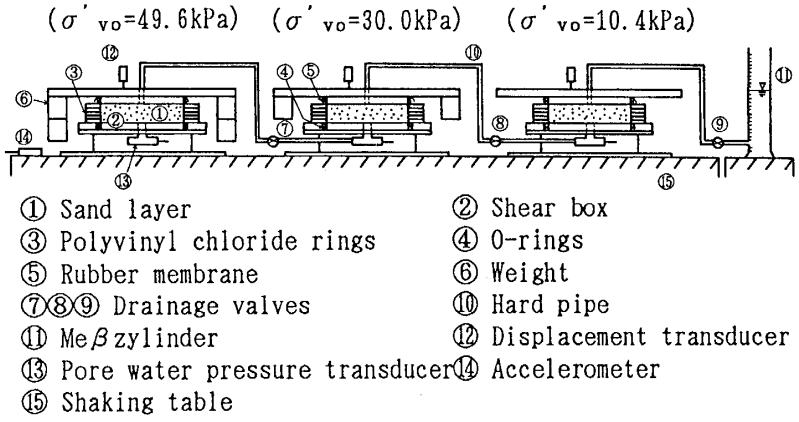

Fig. 5 Three Kjellman's type simple shear boxes fixed on a shaking table

on the surface of the sand layers to apply the required vertical stresses σ'_{vo} to them. The magnitude of σ'_{vo} are 10.4kPa, 30.0kPa and 49.6kPa, respectively, at the bottom of the sand layer.

In order to allow freely to flow pore water in the sand layers to the neighbor sand layers, they were connected with the hard pipes ⑩ in which the pore water was filled. Thus the model (1) was prepared.

Moreover, the models (2)～(5) consisting of two sand layers were also prepared using the same method. The values of σ'_{vo} and RVS of all model sand layers are summarized in Table 1.

Test Procedure

The liquefaction tests using the shaking table were performed on the model as follows. Horizontal sinusoidal vibration with a period T=1/3sec and required constant acceleration amplitude was applied to the model under the undrained conditions. The seismic coefficient k_h used in these tests are 0.09, 0.13, 0.15 and 0.17. Thus, in these tests the magnitude of stress ratio τ/σ'_{vo} applying to the model sand layers during the vibration are nearly equals to k_h. Here τ is the amplitude of cyclic shear stress acting on the bottom of the sand layer.

During the vibration we measured the pore water pressures at the bottom of the sand layers, the amplitude of shear deformation, the change in height of the sand layers and the acceleration of shaking table. The transducers for these measurements were, respectively, the pore water pressure transducers (capacity : 980kPa), the displacement transducers (capacity : 10mm) and the accelerometer (capacity : 5g).

After liquefaction occurred, the vibration was stopped. Then the drainage valve ⑨ was opened, and the amounts of settlement of the sand layers induced by the drainage consolidation were measured.

Moreover, the liquefaction tests were performed on three independent sand layers which were prepared by closing the valves ⑦ and ⑧. These sand layers are referred to as the element sand layers hereafter.

Liquefaction Characteristics of Model (1)

The typical test records of the model (1) which were carried out at $k_h=0.17$ and 0.09 are shown in Figs. 6 (a) and (b), respectively. Also, Fig. 6 (c) shows the typical test record of the element sand layers at $k_h=0.09$. Fig. 6 (a) shows the result that three sand layers of the model (1) liquefied almost simultaneously, and is similar to the test record shown in Fig. 6 (c). On the other hand, Fig. 6 (b) represents the result that the sand layer of $\sigma'_{vo}=10.4$kPa occurred to liquefy, though both sand layers of $\sigma'_{vo}=30.0$kPa and 49.6kPa didn't occur to liquefy.

In this paper, we defined that liquefaction occurred at the time when the pore water pressure induced in the sand layer becomes equal to the value of σ'_{vo}. In these records, the recording lines show the acceleration of shaking table, the shear strain of or volumetric strain of the sand layers and the pore water pressures induced in the sand layers of $\sigma'_{vo}=10.4$kPa, 30.0kPa and 49.6kPa from the top of those figures. ε_v is the amount of the change in height of the sand layer induced during the vibration divided by its initial height and denotes the volumetric strain of the sand layer.

Fig. 7 shows the relationship between the stress ratio τ/σ'_{vo} and the number of cycles required to cause liquefaction n_L for the model (1). Symbol ∞ shown on the right-hand side of Fig. 7 indicates that the sand layer didn't occur to liquefy. For comparison, the test results of the element sand layers are also represented in this figure.

As shown in Fig. 7, the τ/σ'_{vo}-logn_L relation for the element sand layers is shown by a curve irrespective of the magnitude of σ'_{vo}. But strictly speaking, the liquefaction resistances for $n_L=5$, 10 and 20 of the element sand layers decrease very slightly with increasing σ'_{vo} as may be seen in Fig. 8. Fig. 8 was prepared on the basis of the results of the element sand layers shown in Fig. 7 and the others. This result agrees well with the results obtained from other liquefaction tests, which were carried out under confining pressure $\sigma_3 \geqq 49.0$kPa using cyclic triaxial test apparatus[10),11)].

As mentioned above, it is noted in Fig. 7 that in the case of $\tau/\sigma'_{vo}=0.15$ and 0.17, three sand layers of the model (1) liquefied simultaneously at almost the same n_L as that of the element sand layers. In the case of $\tau/\sigma'_{vo} \leqq 0.13$, however, the sand layer of $\sigma'_{vo}=10.4$kPa liquefied at $n_L=18$ which is smaller than n_L for the element sand layer of $\sigma'_{vo}=10.4$kPa, while both sand layers of $\sigma'_{vo}=30.0$kPa and 49.6kPa didn't liquefy. Thus it was clarified that the liquefaction characteristics of three sand layers of the model (1) depend on the magnitude of τ/σ'_{vo}, that is, k_h. This result agrees qualitatively well with the result that the sand layer below the model structure of high vertical stress didn't occur to liquefy, though the sand layer near the model structure of low vertical stress occurred to liquefy[4),7)].

Figs. 9 (a) and (b) show the time histories of the pore water pressures u and the volumetric strains ε_v induced in three sand layers of the model (1) obtained from the test records shown in Fig. 6 (a) and Fig. 6 (b), respectively. Also, Fig. 9 (c) shows the similar curves for the element sand layers obtained from the test record shown in Fig. 6 (c). It is seen from Fig. 9 (a) that in the case of $k_h=0.17$, since n_L is small, all of three sand layers liquefy at almost the same time $t=4.2$sec, namely, $n_L=12$. Furthermore, the pore water pressures induced in three sand layers increase with

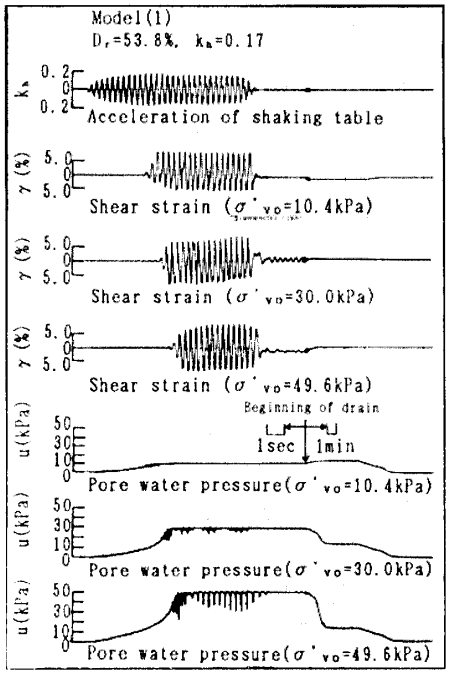

Fig. 6 (a) Typical test record of model (1) ($k_h=0.17$)

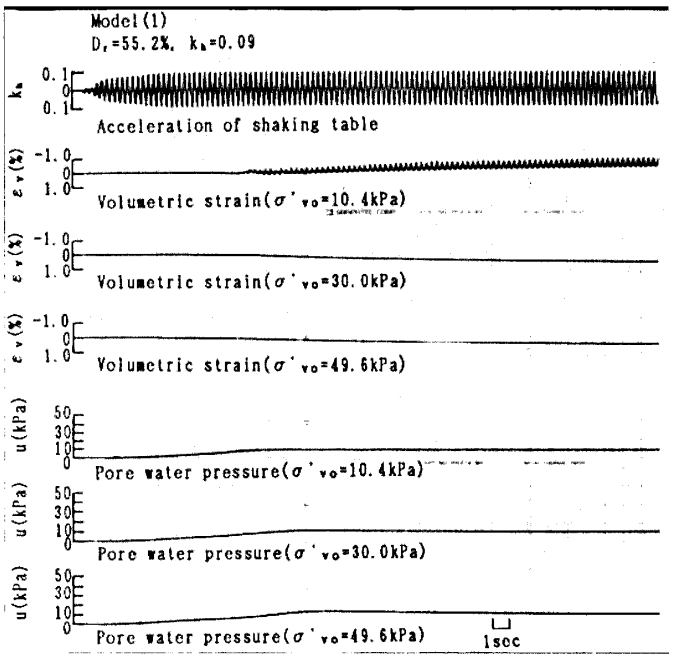

Fig. 6 (b) Typical test record of model (1) ($k_h=0.09$)

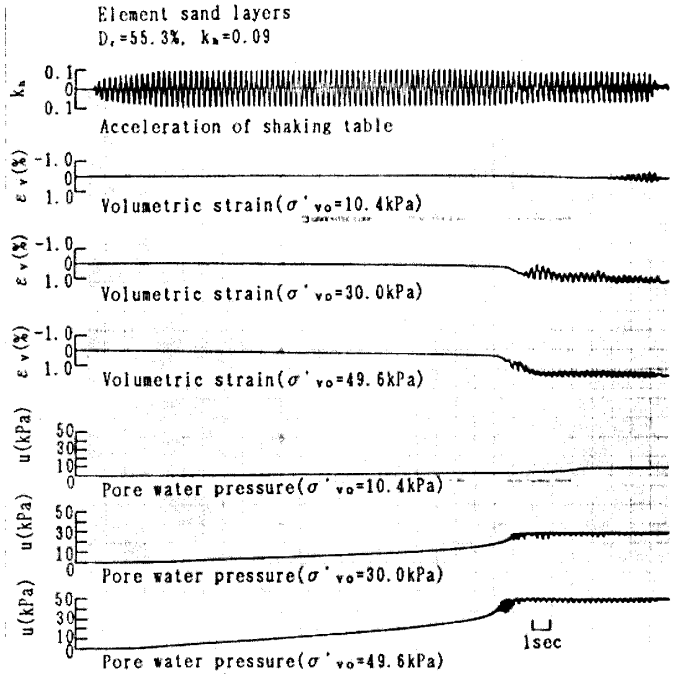

Fig. 6 (c) Typical test record of element sand layers ($k_h=0.09$)

approximately the same amount until the sand layers begin to liquefy. This is because that three sand layers are connected with hard pipe filled with the pore water each other. Similarly it is seen from Fig. 9 (c) that in the case of $k_h=0.09$ the three sand element sand layers liquefied at $n_L=76$ almost simultaneously. But in this case the

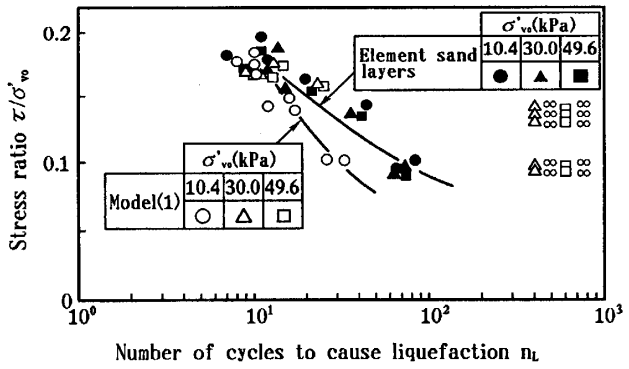

Fig. 7 Liquefaction characteristics of model (1) and element sand layers

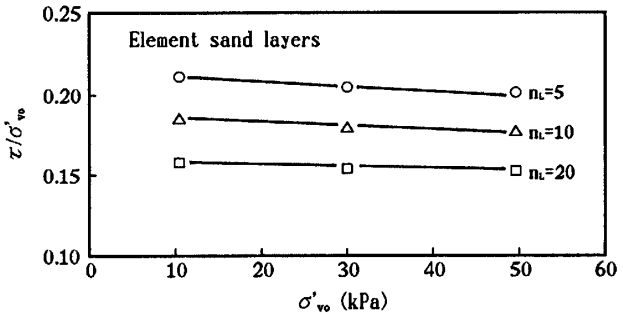

Fig. 8 Effect of effective vertical stress on liquefaction resistance of element sand layers

pore water pressures induced in three element sand layers increase individually.

On the other hand, it is found from Fig. 9 (b) that in the case of $k_h=0.09$ where n_L is small, the pore water pressures induced in three sand layers of the model (1) increase with approximately same rate until the sand layer of $\sigma'_{vo}=10.4$kPa begins to liquefy. As mentioned above, this sand layer of $\sigma'_{vo}=10.4$kPa only liquefies at $n_L=18$, and this n_L is smaller than n_L for the element sand layers. This is because that the pore water pressure induced in the sand layer of $\sigma'_{vo}=10.4$kPa is affected by those induced in the sand layers of $\sigma'_{vo}=30.0$kPa and 49.6kPa.

When the sand layer of $\sigma'_{vo}=10.4$kPa liquefied, its particle structure became loose and the sand layer began to expand due to the pore water flowing from the sand layer of $\sigma'_{vo}=30.0$kPa. Thereafter, the pore water pressures of the sand layers of $\sigma'_{vo}=30.0$kPa and 49.6kPa gradually decrease due to the flowing the pore water to the sand layer of $\sigma'_{vo}=10.4$kPa from those both sand layers. When the sand layer of $\sigma'_{vo}=10.4$kPa liquefied, the pore water pressure ratio u/σ'_{vo} of the sand layer of $\sigma'_{vo}=30.0$ kPa is $10.4/30.0=0.35$ and that of $\sigma'_{vo}=49.6$kPa is $10.4/49.6=0.21$.

By the way, it has been clarified in our previous paper[12] that when u/σ'_{vo} of the sand layer reaches 0.5~0.6, the sand layer should liquefy certainly. This result was also obtained for the element sand layers shown in Fig. 6 (c) and Fig. 9 (c). Therefore, it maybe considered that because the values of u/σ'_{vo} of two sand layers of $\sigma'_{vo}=30.0$ kPa and 49.6kPa of the model (1) don't reach this limited value of $u/\sigma'_{vo}=0.5$ when the sand layer of $\sigma'_{vo}=10.4$kPa liquefies, the former two sand layers never occur to

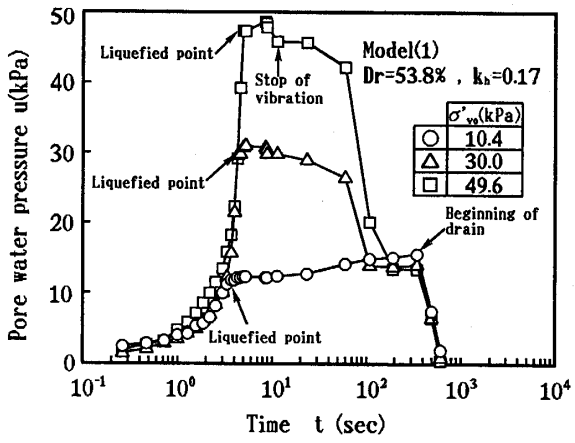

Fig. 9 (a) Typical time history of pore water pressure u of model (1) (k_h = 0.17)

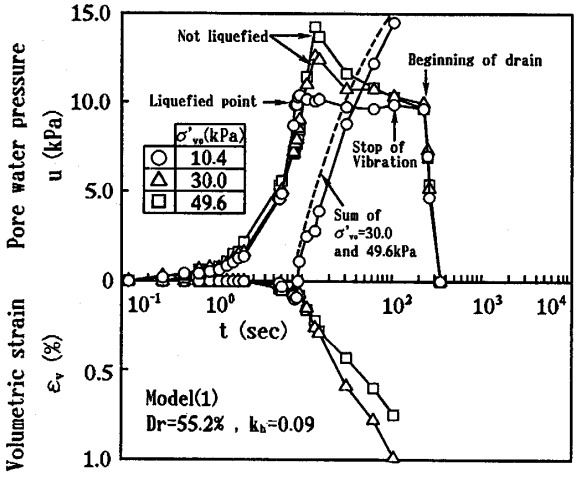

Fig. 9 (b) Typical time histories of pore water pressure u and volumetric strain ε_v of model (1) (k_h=0.09)

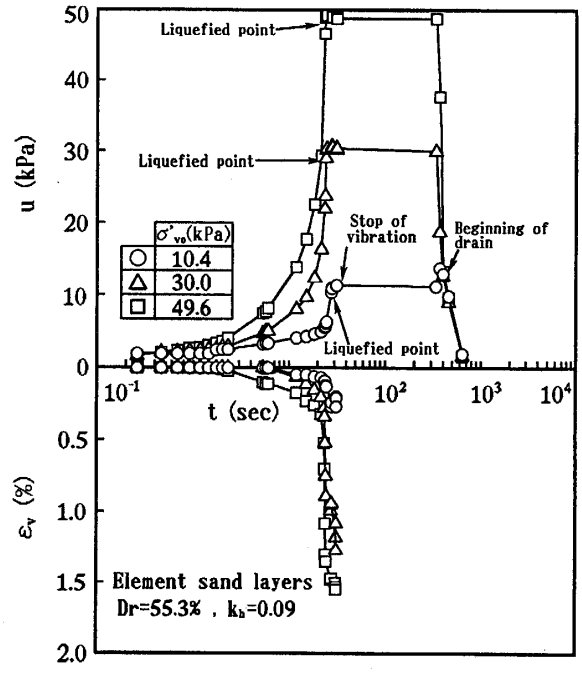

Fig. 9 (c) Typical time histories of u and ε_v of element sand layers (k_h=0.09)

liquefy.

It is seen in Fig. 9 (b) that the amount of expansive strain of the sand layer of σ_{vo} = 10.4kPa shown by the full line is nearly equal to the sum of the compressive strain of the sand layers of σ'_{vo}=30.0kPa and 49.6kPa shown by the dotted line.

After the stop of vibration the pore water pressures of two sand layers of σ'_{vo}=30.0 kPa and 49.6kPa decrease to be equal to that of the sand layer of σ'_{vo}=10.4kPa.

Effect of RVS on Liquefaction Characteristics of Models

In the preceding section, it was clarified that the sand layer of lower vertical stress $(\sigma'_{vo})_s$ in the model (1), that is, that near the structure always liquefies, while the sand layer of higher one $(\sigma'_{vo})_l$, that is, that below the structure does or doesn't liquefy depending on the magnitude of k_h. Next, it was assumed that whether the liquefaction of the sand layer of $(\sigma'_{vo})_l$ will occur or not, will depend on the value of RVS, which was given by Eq. (1).

Because it is very interesting to confirm above reasoning, the liquefaction tests were further performed on four kinds of models (2)~(5) consisting of two sand layers of which the values of RVS differ fairly. The values of RVS of these models are shown in Table 1. For example, the value of RVS of model (1) is 10.4/30.0=0.35 as shown in Table 1.

Fig.10 shows an example of the time histories of u and ε_v of the model (2) with RVS=0.52, which was obtained by the test carried out at $k_h=0.13$. It is noted in this figure that both sand layers liquefied at almost the same time t=9.3sec, namely, $n_L=28$.

The relations between τ/σ'_{vo} and n_L for each sand layer of the models (2)~(5) are shown in Fig.11. Both relation curves for the model (1) and the element sand layers (Fig. 7) are also represented in this figure. As may be seen in this figure, in the case of the models (2) and (5) of which the RVS-values are over about 0.5, the liquefaction characteristics of both sand layers are almost equal to those of the element sand layers. But in the case of the models (3) and (4) of which the RVS-values are below about 0.5, the sand layer of $(\sigma'_{vo})_s$ liquefies easier than the element sand layers, though the sand layer of $(\sigma'_{vo})_l$ doesn't liquefy.

Fig.12 shows the relation between the maximum pore water pressure ratio $(u/\sigma'_{vo})_{max}$ induced in the sand layer of $(\sigma'_{vo})_l$ and the RVS-value obtained from the tests on the models (1)~(5). All data are of those obtained for $k_h \leqq 0.13$. The test results obtained by Yoshimi and Tokimatsu[4] and Ishihara and Matsumoto[7] are also rearranged in this figure, referring to Figs. 1 and 2.

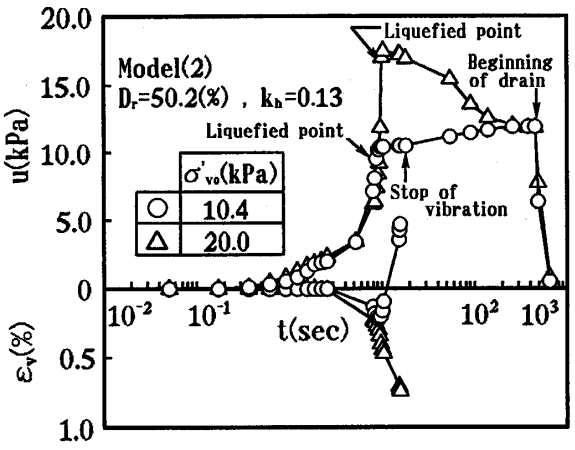

Fig.10 An example of time histories of u and ε_v of model (2)

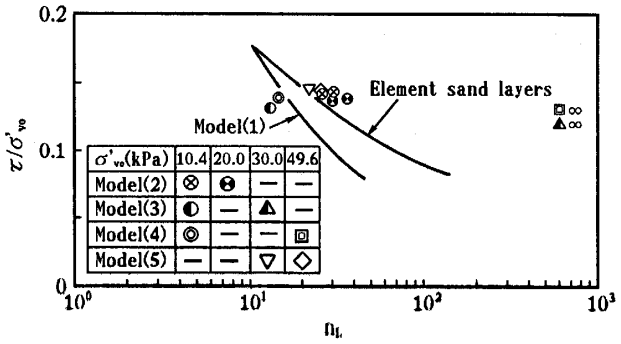

Fig.11 Liquefaction characteristics of models (2), (3), (4) and (5)

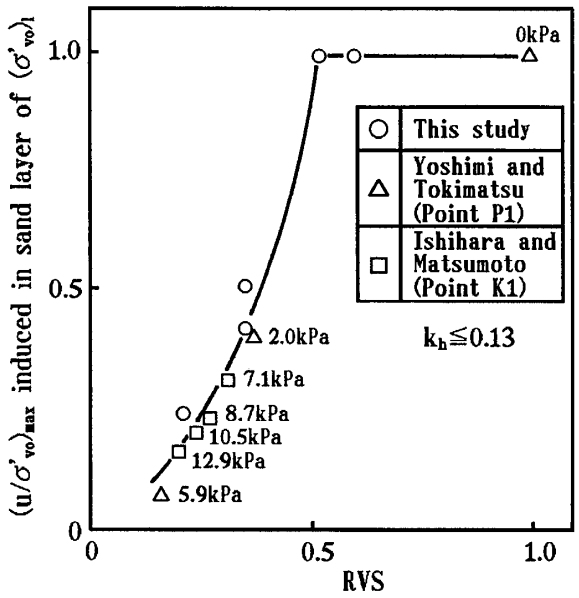

Fig.12 Relation between $(u/\sigma'_{vo})_{max}$ induced in the sand layer of $(\sigma'_{vo})_1$ and RVS

It is noted in Fig.12 that, although there was complete differences in the kind of sand, the density of the sand layer, the test equipment and the test condition between three tests, the relation between $(u/\sigma'_{vo})_{max}$ and RVS is given by a unique curve. It is also noted in Fig.12 that when the RVS-values are below about 0.5, the values of $(u/\sigma'_{vo})_{max}$ of all sand layers don't reach 1.0, that is, they don't occur to liquefy.

On the basis of the above results, it can be concluded that the liquefaction characteristics of the saturated sand layers of which vertical stresses are quite different partially, is affected by the values of RVS and k_h.

It was found that in the case of $k_h \leqq 0.13$ the pore water pressures induced in the sand layers increase in proportion to the number of shear cycles n until u/σ'_{vo} reaches 0.5~0.6. So, we defined the a-value by Eq. (2) as an index indicating the rate of increase of pore water pressures, and examined the relation of a-value and k_h for the model sand layers.

$$a = (u/\sigma'_{vo})/(n/n_L) \qquad (2)$$

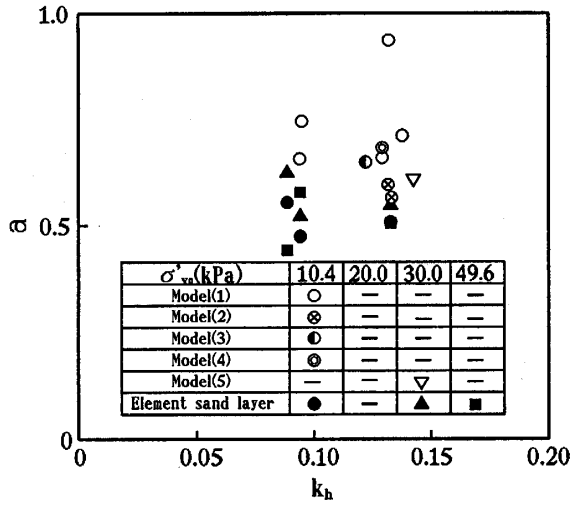

Fig.13 Relation between a-value and k_h for model sand layers and element sand layers

The result is represented in Fig.13. It is seen in Fig.13 that the a-values of all sand layers of $\sigma'_{vo}=10.4$kPa of the model (1) are over 0.65 and are considerably larger than those of all element sand layers. Also, as mentioned above, the increases of the pore water pressures induced in the sand layers of $(\sigma'_{vo})_S$ are influenced by the pore water pressures induced in the sand layers of $(\sigma'_{vo})_1$.

Liquefaction-Induced Settlements of Model (1)

We measured the amount of settlements of three individual sand layers of model (1) caused by the drainage consolidation after liquefaction. The relation between the volumetric strain ε_v and k_h for three sand layers is shown in Fig.14(a). Also, the same relation for the element sand layers is shown in Fig.14(b). As may be seen in both figures, considerable scatter in the values of ε_v for each k_h is recognized. This is due to the difference of the shaking time during liquefaction t_{LS}. Namely, t_{LS} for the model (1) and the element sand layers are in the range of 4.5~9.7sec and 4.3~9.5sec, respectively. It has been clarified in our previous study[14] that the value of ε_v increases with increasing t_{LS}. Therefore, the relation between ε_v and k_h for the sand layer of each σ'_{vo} should be given with the shadowed portion.

It is found from Figs.14(a) and (b) that the amount of ε_v of each sand layer increases with increasing k_h. Also, when the value of k_h is the same, the volumetric strain of each sand layer increases as its vertical stress increases. This is because that since inertia forces acting the sand layers during the vibration becomes larger as the vertical stress increases, the sand layers were more densified by the drainage after liquefaction.

It can be read from Fig.14(a) that ε_v induced in the sand layers of $\sigma'_{vo}=30.0$kPa and 49.6kPa of the model (1) which was not liquefied at k_h in the range of 0.09~0.13, is 0.5% to 1.7%. This value is significantly smaller than ε_v in the range of 2.3~4.6% (in case of $k_h=0.09$) to in the range of 3.1~5.3% ($k_h=0.13$) induced in the element

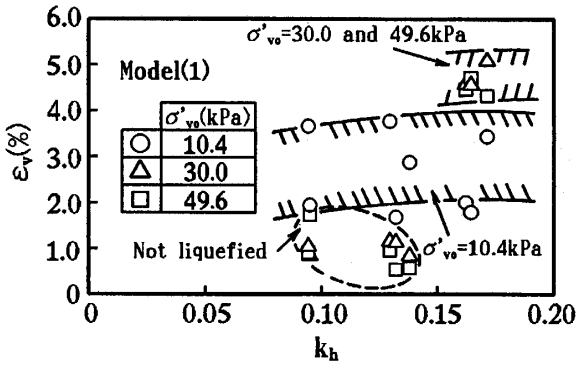

Fig.14(a) Relation between volumetric strain ε_v caused by liquefaction and k_h (model (1))

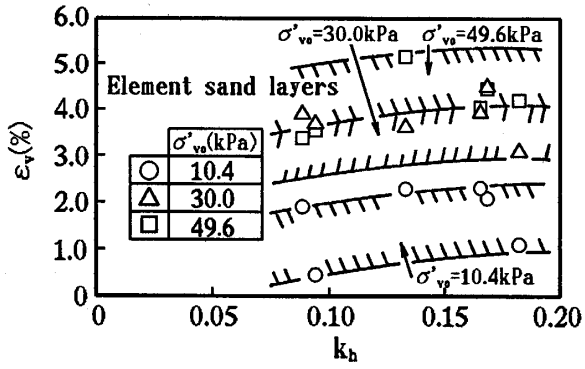

Fig.14(b) Relation between volumetric strain ε_v caused by liquefaction and k_h (element sand layers)

sand layers of the same vertical stresses liquefied (Fig.14(b)).

Fig.15 shows the relation between the liquefaction-induced volumetric strain ε_v for the model (1) and the vertical stress σ'_{vo} at $k_h=0.09$, 0.13 and 0.17 obtained from the result shown in Fig.14(a). It is seen from this figure that in the case of $k_h=0.17$ the liquefaction-induced volumetric strain ε_v of the sand layers increases rapidly up to for $\sigma'_{vo}=30.0$kPa and takes a constant value of 5 % for over its vertical stress.

Conclusions

The characteristics of liquefaction and liquefaction-induced settlements of saturated sand deposits of which the vertical stresses are different partially such as those below and near embankments and structures are studied experimentally. The model (1) consisting of three sand layers was prepared in three Kjellman's type shear boxes, and the liquefaction tests on it were performed using the shaking table. The vertical stresses σ'_{vo} applied to each sand layer are 10.4kPa, 30.0kPa and 49.6kPa. For comparison, the same tests were carried out on four kinds of models (2)~(5) consisting of two sand layers of which a combination of the vertical stresses differs fairly.

The conclusions obtained by these tests are summarized as follows. The liquefaction characteristics of the model sand layers depend on the ratio of vertical stresses RVS as well as the seismic coefficient k_h. Namely, in the case of $k_h \geqq 0.15$, irrespective of the RVS-values and in the case of $k_h<0.15$ and RVS$\geqq$0.5, all sand layers of the models have the same liquefaction characteristics as those of the element sand layers. One the contrary, in the case of $k_h<0.15$ and RVS$<$0.5, the sand layer of lower vertical stress liquefied considerably faster than the element sand layers due to the effect of pore water pressure induced in the sand layers of higher vertical stress, though the sand layers of higher vertical stress didn't occur to liquefy.

In other words, because the number of shear cycles to cause liquefaction becomes larger in the case of small k_h, unless the pore water presure ratios u/σ'_{vo} of the sand layers of $\sigma'_{vo}=30.0$kPa and 49.6kPa reach about 0.5 when the sand layer of $\sigma'_{vo}=$

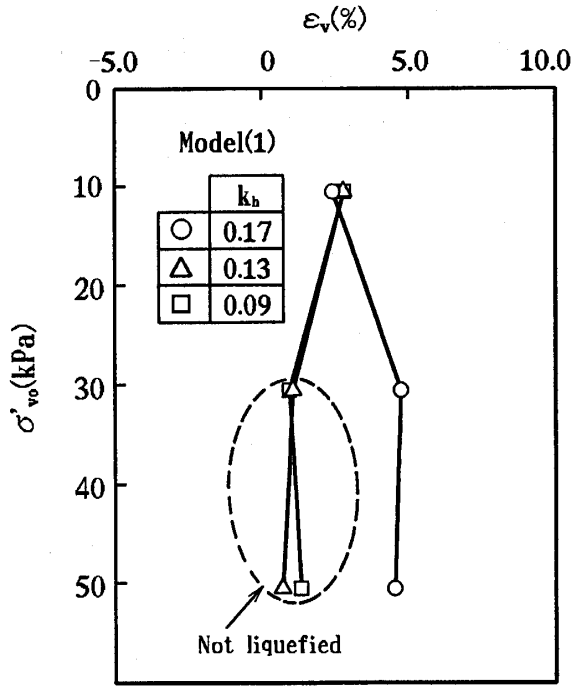

Fig.15 Relation between volumetric strain ε_v caused by liquefaction and vertical stress σ'_{vo} for model (1)

10.4kPa liquefies, the pore water pressures of the former sand layers decrease gradually due to remarkable expansion of the latter sand layer produced after its liquefaction, and finally the former sand layers don't liquefy.

The liquefaction-induced settlements of the model (1) at $k_h=0.17$ are that the amount of volumetric strain increases remarkably up to for $\sigma'_{vo}=30.0$kPa and takes a constant value of 5 % for over its vertical stress.

Acknowledgments

The authors would like to express their gratitude to Messrs. Hiroshi Yurino and Yoshinobu Shimahara, the former students at the Yamaguchi University, for their helps during the experiments and the arrangements of the test results.

References

1) Fact-finding committee on the Niigata earthquake damage of JSCE: "Report on Investigation on the Shyowa 39 Year Niigata Earthquake Damages," Japan Society of Civil Engineers (1966) (in Japanese)

2) Seed, H. B., Lee, K. L., Idriss, I. M. and Makdisi, F. I.: "The Slides in the San Fernando Dam during the Earthquake of February 9, 1971, "Journal of the Geotechnical Engineering Division, ASCE, **101** [GT7], 651-688 (1975)

3) Sasaki, Y., Taniguchi, E., Matsuo, O. and Ito, Y.: "Settlement of Earth Structures Caused by the Nihonkai-Chubu Earthquake,"Tsuchi-to-Kiso, **32** [9], 7-12 (1984) (in Japanese)

4) Yoshimi, Y. and Tokimatsu, K.: "Liquefaction of Sand near Structures during Earthquakes,"

Proc. of the 4th Japan Earthquake Engineering Symposium, 439-446 (1975) (in Japanese)
5) Yoshimi, Y. and Tokimatsu, K.: "Settlement of Buildings on Saturated Sand during Earthquakes," Soils and Foundations, **17** [1], 23-38 (1977)
6) Yoshimi, Y. and Tokimatsu, K.: "Two-dimensional Pore Pressure Changes in Sand Deposits during Earthquakes," Proc. of 2nd International Conference on Microzonation, **2**, 853-863 (1978)
7) Ishihara, K. and Matsumoto, K.: "Bearing Capacity of Saturated Sand Deposits during Vibration," Proc. of the 4th Japan Earthquake Engineering Symposium, 431-438 (1975) (in Japanese)
8) Koga, Y. and Matsuo, O.: "Shaking Table Tests on Embankments Resting on Liquefiable Sandy Ground," Soils and Foundations, **30** [4], 161-174 (1990)
9) Abe, H. and Kusano, K.: "Shaking Table Tests on Level Ground and Embankment," Annual Report I.C.E. of TMC, 257-266 (1991) (in Japanese)
10) Tatsuoka, F., Iwasaki, T., Tokida, K. and Kon-no, M.: "Cyclic Undrained Triaxial Strength of Sampled Sand Affected by Confining Pressure, "Soils and Foundations, **21** [2], 115-120 (1981)
11) Yunoki, Y., Ishihara, K., Seki, M. and Yoneda, Y.: "Effect of Initial Effective Confining Pressure on the Behavior of Cyclic Triaxial Shear of Dense Sand," Proc. of the 17th Japan National Conference on Soil Mechanics and Foundations Engineering, 1649-1652 (1982) (in Japanese)
12) Ōhara, S. and Yamamoto, T.: "Correlation between Stationary and Damped Vibration Waves Required to Cause Liquefaction of Sand," Tsuchi-to-Kiso, **36** [12], 31-36 (1988) (in Japanese)
13) Ōhara, S. and Yamamoto, T.: "Coefficient of Earth Pressure of Sand during Cyclic Shear," Proc. of Japan Society of Civil Engineers, 412, 89-97 (1989) (in Japanese)
14) Ōhara, S. and Yamamoto, T. and Yurino, H.: "Experimental Study on Reliquefaction Potential of Saturated Sand Deposit," Proc. of the 10th World Conference on Earthquake Engineering, III, 1425-1430 (1992)